Contactless Determination of Electrical Conductivity of One-Dimensional Nanomaterials by Solution-Based Electro-orientation Spectroscopy

Cevat Akin,[†] Jingang Yi,[†] Leonard C. Feldman,[‡] Corentin Durand,[§] Saban M. Hus,[§] An-Ping Li,[§] Michael A. Filler,[⊥] and Jerry W. Shan*[,†]

[†]Department of Mechanical and Aerospace Engineering and [‡]Institute of Advanced Materials, Devices, and Nanotechnology, Rutgers University, Piscataway, New Jersey 08854, United States, [§]Center for Nanophase Materials Sciences, Oak Ridge National Laboratory, Oak Ridge, Tennessee 37831, United States, and [⊥]School of Chemical & Biomolecular Engineering, Georgia Institute of Technology, Atlanta, Georgia 30332, United States

ABSTRACT Nanowires of the same composition, and even fabricated within the same batch, often exhibit electrical conductivities that can vary by orders of magnitude. Unfortunately, existing electrical characterization methods are time-consuming, making the statistical survey of highly variable samples essentially impractical. Here, we demonstrate a contactless, solution-based method to efficiently measure the electrical conductivity of 1D nanomaterials based on their transient alignment behavior in ac electric fields of different frequencies. Comparison with direct transport measurements by probe-based scanning tunneling microscopy shows that electro-orientation spectroscopy can quantitatively measure nanowire conductivity over a 5-order-of-magnitude range, 10^{-5}–$1\ \Omega^{-1}\ m^{-1}$ (corresponding to resistivities in the range 10^{2}–$10^{7}\ \Omega \cdot cm$). With this method, we statistically characterize the conductivity of a variety of nanowires and find significant variability in silicon nanowires grown by metal-assisted chemical etching from the same wafer. We also find that the active carrier concentration of n-type silicon nanowires is greatly reduced by surface traps and that surface passivation increases the effective conductivity by an order of magnitude. This simple method makes electrical characterization of insulating and semiconducting 1D nanomaterials far more efficient and accessible to more researchers than current approaches. Electro-orientation spectroscopy also has the potential to be integrated with other solution-based methods for the high-throughput sorting and manipulation of 1D nanomaterials for postgrowth device assembly.

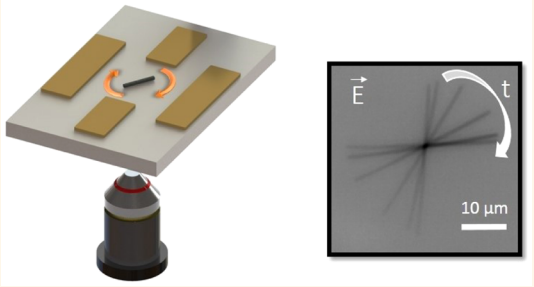

KEYWORDS: electro-orientation · electrical conductivity measurement · nanowires · nanotubes · postgrowth sorting

Nanowires are not all the same. Those of the same composition or even within the same batch can vary by orders of magnitude in electrical properties for a variety of fundamental and practical reasons: (1) The number of surface traps can far exceed the number of charge carriers in the volume of a nanowire, rendering the nanowire's electronic properties highly sensitive to surface variation and treatment. (2) Doping uncertainty can lead to sample-to-sample variation, with even six-nines-pure (99.9999%) catalyst particles able to cause unwanted doping levels and traps. (3) Within a given sample, wafer- or chamber-wide variation in growth conditions can cause individual nanowires to differ widely. (4) More fundamentally, intrinsic statistical variations can arise from discrete numbers of charge carriers.[1] [For example, lightly doped Si nanowires of diameter 10 nm and length 1 μm with carrier concentration 10^{16} atoms/cm^3 will have an average of just 0.8 dopant atom per nanowire.] Even a single point defect can cut off a nanowire and lead to a metal–insulator transition.[2] Thus, not only do nanowire transport properties differ significantly from that of their bulk counterparts because of surface and quantum-size effects,[3] but also the properties of individual nanowires can be expected to have an inherent variability.

For this reason, it is important to be able to statistically characterize the electrical properties of 1D nanomaterials. Electrical-transport measurements using nanoprobes

* Address correspondence to jshan@jove.rutgers.edu.

Received for review February 20, 2015 and accepted May 5, 2015.

Published online May 05, 2015
10.1021/acsnano.5b01170

under SEM[4] or microfabricated electrodes[5] are slow and laborious. This inefficiency makes direct-contact measurements poorly suited for the large number of measurements needed to statistically characterize variations. Other available techniques such as atom probe tomography,[6,7] scanning photocurrent microscopy (SPCM),[8] Kelvin probe force microscopy (KPFM),[9,10] and electron holography[11] can find doping distribution and carrier-density profiles along nanowires, but are similarly slow and cannot provide statistical information about the entire ensemble.

Here, we introduce and validate an efficient method for the rapid, contactless, and quantitative determination of electrical conductivity of 1D nanomaterials. With assumptions about the carrier mobility, the active carrier concentration in the nanowires can also be found. The method is based upon the direct optical visualization of the frequency-dependent alignment rates of nanowires when they are suspended in a liquid of known properties and subjected to spatially uniform ac electric fields of different frequency. The electro-orientation-spectroscopy method is demonstrated on Si, Al_2O_3, and TiO_2 nanowires with diameters between 100 and 300 nm and lengths of 5−30 μm. In principle, the technique can be applied to 1D nanomaterials as small as single-wall carbon nanotubes (SWNTs), whose dynamics in liquid suspensions have been optically visualized by several groups.[12−14] Because it is rapid, taking only minutes to measure the electrical conductivity of a nanowire, electro-orientation spectroscopy provides a unique tool for statistical characterization of 1D nanomaterials having significant variability in electrical properties.

The general manipulation of particles *via* electrokinetic techniques such as dielectrophoresis, electrorotation, and electro-orientation has been extensively studied.[15−17] In the case of electro-orientation, the electric field induces a dipole moment in the freely suspended nanowire or nanotube that causes it to rotate into alignment with the field.[18,19] The induced dipole moment causing the alignment is a strong function of the electrical properties of the particle and the frequency of the applied field (see Supporting Information). Figure 1 shows the alignment rates predicted for Maxwell−Wagner interfacial polarization[18] for nanowires under different ac electric fields. There is a transition range of frequencies where the transient rotation rate differs for 1D nanomaterials of different electrical properties. In particular, the alignment rate at low frequencies depends on the conductivity difference between the nanowire and solvent, while the alignment rate at higher frequencies depends on permittivities. The crossover frequency, $\omega_{crossover}$, for the transition is given by the inverse of the Maxwell−Wagner time scale, $\tau_{mw_{||}}$, which for 1D nanomaterials is

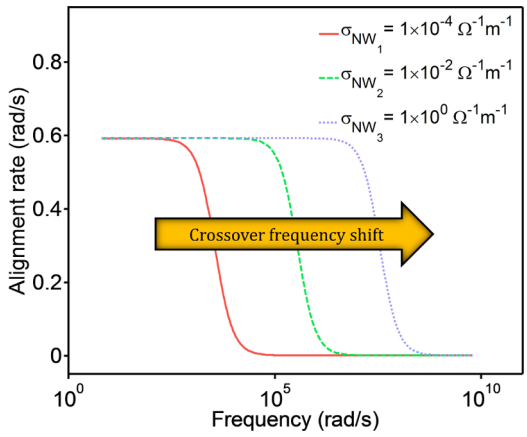

Figure 1. Shift in electro-orientation crossover frequency with particle conductivity. The alignment rate for oil-suspended 1D nanomaterials varies with the frequency of the applied electric field, with the shift in crossover frequency with particle conductivity allowing noncontact measurement of the electrical properties of nanowires and nanotubes. Curves are plotted for Maxwell−Wagner interfacial polarization of Si nanowires (diameter of 150 nm, length of 10 μm) of different conductivity suspended in light-viscosity mineral oil ($\varepsilon_f = 2.0 \times 10^{-11}$ F/m, $\sigma_f = 1.0 \times 10^{-10}$ Ω^{-1} m^{-1}, μ = 25.9 cP).

$$\omega_{crossover} = \frac{1}{\tau_{mw,||}} = \frac{(1 - L_{||})\sigma_f + \sigma_p L_{||}}{(1 - L_{||})\varepsilon_f + \varepsilon_p L_{||}} \quad (1)$$

where σ is the conductivity, ε is the permittivity, $L_{||}$ is the geometric depolarization factor, and the subscripts f and p refer to the fluid and particle, respectively. For high-aspect-ratio particles, the depolarization factor simplifies to $L_{||} \simeq (1/(\beta^2))[\ln 2\beta - 1]$, where β is the aspect ratio of the 1D nanomaterial. In the limit of high-aspect-ratio 1D nanomaterials and a low-conductivity solvent, the depolarization factor becomes very small (*e.g.*, $L_{||} \lesssim 10^{-3}$ for $\beta \gtrsim 50$) and the crossover frequency simplifies to

$$\omega_{crossover} \cong \frac{\sigma_p}{\varepsilon_f(L_{||}^{-1} - 1)} \quad (2)$$

It is important to note that the crossover frequency then depends only on the particle conductivity and fluid permittivity and not on the (also unknown) particle permittivity. Thus, by measuring the alignment behavior of the nanowires at different frequencies in a fluid of known permittivity, we can extract the electro-orientation crossover frequency and quantitatively measure the effective electrical conductivity of the 1D nanostructures. This analysis assumes that the nanoparticle and surrounding fluid can be treated as polarizable lossy dielectrics with homogeneous (effective) electrical properties.[18]

RESULTS AND DISCUSSION

We have developed and validated this electro-orientation-spectroscopy method using a variety of insulating and semiconducting 1D nanomaterials ranging over 5 orders of magnitude in electrical

TABLE 1. Statistics of the Measured Electrical Conductivities of Different Nanowire Samples

nanowire type	mean and standard deviation of the mean of electro-orientation spectroscopy (Ω^{-1} m^{-1})	minimum and maximum of electro-orientation spectroscopy (Ω^{-1} m^{-1})
as-produced Si	$(4.1 \pm 0.8) \times 10^{-2}$ (18 nanowires)	min: 0.7×10^{-2} max: 7.5×10^{-2}
passivated Si	$(4.4 \pm 0.6) \times 10^{-1}$ (22 nanowires)	min: 0.9×10^{-1} max: $\sigma \gg 12 \times 10^{-1}$
Al_2O_3	$(6.2 \pm 2.2) \times 10^{-5}$ (10 nanowires)	min: 0.4×10^{-5} max: 18×10^{-5}
TiO_2	$(1.3 \pm 0.3) \times 10^{-1}$ (20 nanowires)	min: 1.1×10^{-1} max: 3.1×10^{-1}

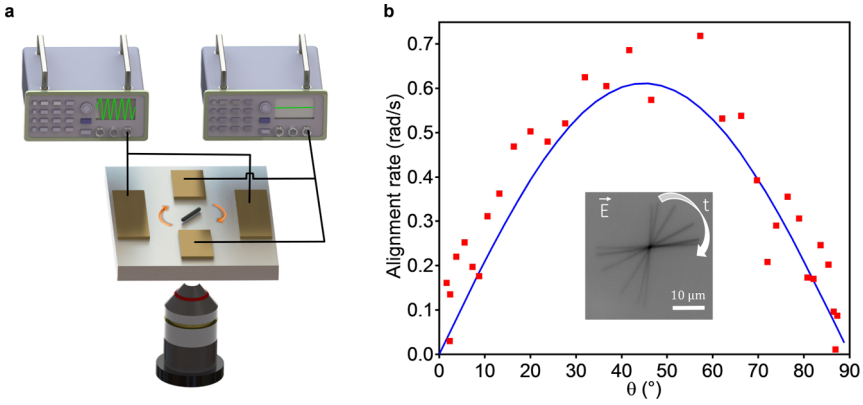

Figure 2. Apparatus and demonstration of alignment. (a) Schematic of experimental setup to measure the electro-orientation spectra of 1D nanomaterials. Horizontal electrodes apply uniform electric fields of different frequencies to induce alignment, while vertical electrodes reorient the nanowires for repeated measurements at different frequencies. (b) Experimentally measured alignment rate of a Si nanowire as a function of angle with electric field. Excellent agreement is found with theoretical predictions with no adjustable constants. Inset: Overlay of images showing time series of nanowire alignment with horizontal electrical field (E = 75 V/mm, $\omega = 2\pi \times 10^2$ rad/s, $\varepsilon_f = 2.0 \times 10^{-11}$ F/m, p = 150, μ = 25.9 cP; see Supporting Information for video).

conductivity (Table 1). Silicon nanowires (diameter: 50−300 nm, length: 5−30 μm) were fabricated using metal-assisted chemical etching of doped Si wafers[20] (see Supporting Information for details), while other nanowires were commercially sourced. The nanowires were measured either as-produced (after annealing in vacuum) or with dry-oxygen passivation at 950 °C. All nanowires used in the experiments were dispersed in mineral oil, placed on a glass slide with four electrodes, and visualized under bright-field illumination on an inverted optical microscope (Figure 2a; see Supporting Information for further experimental details). Mineral oil was chosen to suspend the nanowires because its low conductivity enables the simplification of eq 1, as well as yielding a thick electrical double layer around the particles, which minimizes induced-charge electro-osmotic flow at the particle−fluid interface.[17,21,22] The high viscosity of mineral oil also reduces the disturbances of any possible ac electro-osmotic flow[17,23] on the alignment rates, particularly at low frequencies. We note that flow disturbances affect the measurement only if vorticity is generated; translational background flow has no effect on the method.

The transient alignment rate of a Si nanowire was first recorded under a spatially uniform, low-frequency ac electric field and compared to the theoretically predicted alignment rate. The theoretical alignment rate in the low-frequency limit is independent of particle conductivity (*cf.* Figure 1) and thus can be calculated with no assumptions about the particle properties. As seen in Figure 2b, the alignment rates for a given frequency ($\omega = 2\pi \times 10^2$ rad/s) agree well in both magnitude and angular dependence [$\sin(2\theta)$] with the theory, which has no adjustable constants. Then, to obtain the electro-orientation spectra and determine the electrical properties using eq 2, different ac frequencies were applied to the Si nanowire. As seen in Figure 3a, the measured alignment rate for an individual Si nanowire shows the expected crossover behavior with varying frequency. A mean crossover frequency was obtained by fitting a curve to the data in the form of $\Omega = 1/[1 + (\omega/\omega_{crossover})^2]$ where Ω is the normalized alignment rate, ω is the frequency of the applied electric field, and $\omega_{crossover}$ is the fitted crossover frequency. The fitted crossover frequency is highly sensitive to conductivity differences between nanowires (see Supporting Information Figure S1). The

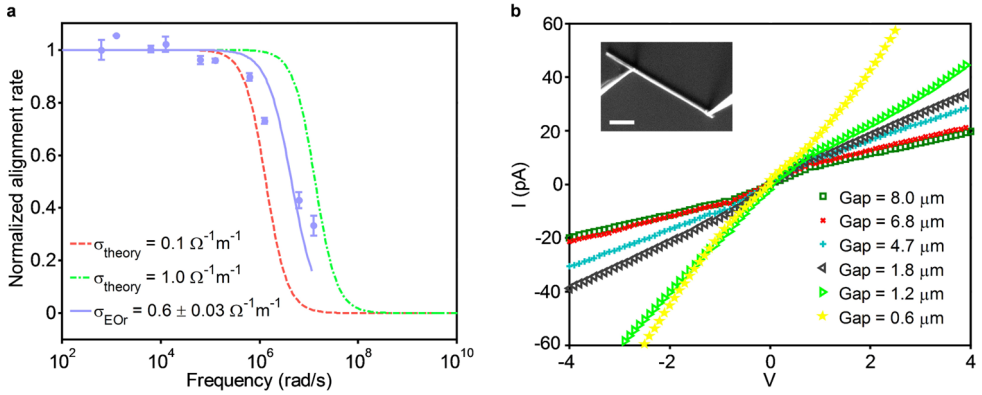

Figure 3. Electro-orientation spectra and 2P-STM measurements. (a) Measured alignment rates of an individual Si nanowire with respect to applied electric-field frequency. The narrow error bars show the low variation in five repeated measurements of the same nanowire. The solid line is a curve fit of the form $\Omega = 1/[1 + (\omega/\omega_{crossover})^2]$, from which the crossover frequency (and hence the nanowire conductivity) can be extracted. Dashed lines are theoretical predictions for different conductivities (Supporting Information). (b) Direct-contact STM measurements of the *I*−*V* curves with different probe spacings (Supporting Information). Inset: SEM image showing a Si nanowire being measured by STM probes.

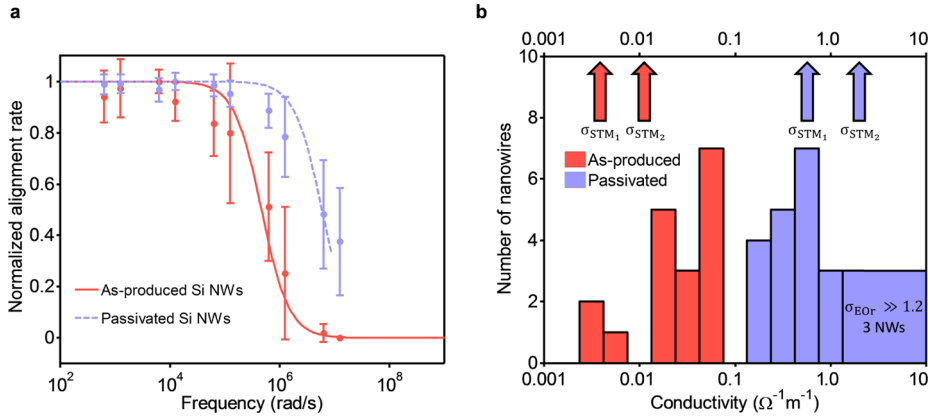

Figure 4. Conductivity measurements of n-type, MACE-grown Si nanowires. (a) Averaged electro-orientation spectra of as-produced and passivated Si nanowires. The larger error bars show the conductivity variations in different nanowires from the same sample (*cf.* the small error bars in Figure 3a for the repeated meaurements of the same nanowire). (b) Measured conductivity distribution of as-produced and passivated Si nanowires obtained with electro-orientation spectroscopy. Arrows show electrical conductivity of four individual as-produced and passivated Si nanowires from the same batch measured *via* direct 2P-STM.

nanowire conductivity can then be found using eq 2. It is important to note that the measured rotation rates show excellent repeatability when the same nanowire is measured more than once, with the small error bars in Figure 3a indicating the uncertainty interval for five repeated measurements.

For n-type Si nanowires, fabricated using metal-assisted chemical etching of a p-doped Si wafer[20] (see Supporting Information for details) we investigated the electro-orientation spectra of 18 individual, as-produced Si nanowires from the same sample at electric-field frequencies ranging from 500 rad/s to 5×10^6 rad/s. The crossover frequency for each nanowire was found, along with the conductivity. Figure 4a shows the averaged electro-orientation spectrum for the set of 18 different nanowires. The larger error bars for mean alignment rates of the samples are due to the variations in conductivity of these nanowires (*cf.* the small error bars in Figure 3a for repeated measurements of the same nanowire). As shown in the histogram of Figure 4b, the distribution of measured conductivities for this set of sample is broad, with two slight peaks at 2×10^{-2} and 6×10^{-2} Ω^{-1} m^{-1}. For comparison, we measured two nanowires from the same sample using two- and four-probe scanning tunneling microscopy (2P/4P-STM) (Figure 3b).[4] Comparisons between two-probe and four-probe measurements showed that the contact resistance of the probes was negligible and that measurements could be made with only two probes because of the low conductivity of the nanowires. Joule heating was also negligible, and photoconductivity was estimated to only weakly contribute to the measured conductivity of the Si nanowires, as discussed in the Supporting Information. Characteristic *I*−*V* curves are shown in Figure 3b for different probe spacings. The conductivity values for two nanowires measured by 2P-STM fall within the range of values measured by

electro-orientation spectroscopy, as indicated by the arrows in Figure 4b. Consistent with the electro-orientation results, the STM measurements also show a large variation in nanowire conductivity, with the two measured nanowires differing by an order of magnitude from each other (0.4 and 1.1 $\times$ 10^{-2} Ω^{-1} m^{-1}).

Despite the good agreement between the electro-orientation and the STM measurements of the as-produced Si-nanowire sample, we noticed that the conductivities were 2 orders of magnitude lower than that of the original bulk Si wafer, whose bulk conductivity was measured to be (2−3.3) $\times$ 10 Ω^{-1} m^{-1}. This difference from the bulk conductivity was hypothesized to come from strong surface effects, as is typical of nanomaterials. To study the influence of surface state on the nanowires, we next investigated Si nanowires with a dry-oxygen surface passivation, which can suppress surface traps. Electro-orientation-spectroscopy measurements were made on 22 individual, passivated Si nanowires. As seen in Figure 4b, passivation increases the effective conductivity of the Si nanowires made from the same wafer by more than an order of magnitude, with a peak around 0.6 Ω^{-1} m^{-1} in the histogram. Similarly, STM-transport measurements on two passivated Si nanowires also showed a more than an order of magnitude increase in conductivity (0.6 and 2 Ω^{-1} m^{-1}). The good agreement between the electro-orientation and STM measurements for the passivated Si nanowires is a further validation of the accuracy of the electro-orientation method. It should be noted that, out of the 22 passivated nanowires that were studied with electro-orientation, three of them had conductivities higher than can presently be measured by the method ($\sigma_{EOr} \gg 1.2\ \Omega^{-1}\ m^{-1}$). The effective measurement range of electro-orientation spectroscopy, and prospects for expanding it, will be discussed later.

The large variation between Si nanowires in the same sample, whether passivated or not, can arise from several causes. First, processing variations and possible impurities introduced during the fabrication of the nanowires may contribute the sample variations measured *via* both electro-orientation and 2P-STM. Second, variations in surface properties and the limited number of dopants may introduce statistical variations from wire to wire. Third, as will be discussed in detail later, geometrical differences between nanowires, which cannot be fully resolved *via* optical microscopy, may cause additional variations in the electro-orientation measurement. It is important to note, however, that the geometric differences (*e.g.*, uncertainty in nanowire diameter) cannot completely account for the variation in nanowire conductivity, since the 2P-STM measurements, which fully resolve the nanowire diameter using SEM, also show order-of-magnitude variations between individual nanowires within the same sample.

Having shown the variability of the Si nanowires, as well as the validity of the electro-orientation method by comparison with direct-contact STM measurements for both as-produced and passivated Si nanowires, we now report on several commercially available 1D nanomaterials. Although the properties of these nanowires are typically not available due to the specialized equipment and laborious effort required to characterize them, it is nonetheless desirable to measure (and sort, if necessary) them for optimal device performance. We have thus applied the electro-orientation-spectroscopy method to characterize commercially available semiconducting and insulating nanowires, namely, Al_2O_3 nanofibers and TiO_2 nanowires. Table 1 summarizes the results of the electro-orientation-spectroscopy measurements on the various 1D nanomaterials. The Al_2O_3 samples showed large variability, with an order-of-magnitude difference between minimum and maximum conductivity, while the TiO_2 nanowires showed less variation. Direct 2P- and 4P-measurements of the conductivity of insulating nanowires are often not reliable due to the difficulty in establishing an ohmic probe−sample contact. However, these 1D nanomaterials could be readily measured with electro-orientation spectroscopy.

The electro-orientation-spectroscopy method is distinct in a number of ways from prior work on characterizing and sorting 1D nanomaterials using solution-based methods. First, while a number of solution-based techniques exist to sort SWNTs based on their chiralities, including selective adsorption,[24,25] polymer and DNA wrapping,[26,27] and density-gradient ultracentrifugation,[28] these methods are not generally applicable to other 1D nanomaterials. Second, related solution-based electrical techniques such as dielectrophoresis[29] and electrorotation[22] have not been compared with direct-contact measurements. The latter has also been reported to suffer from induced-charge electro-osmosis (arising from the motion of the thin electrical double layer of the aqueous solvent), which may limit its quantitative accuracy.[17] Finally, electro-orientation spectroscopy is distinct in having been demonstrated to be capable of detecting surface effects on the electrical transport properties of nanowires.

The measurement range of the electro-orientation technique depends on the properties of the medium and the available bandwidth of the electronics. Figure 5 shows the expected crossover frequency *versus* nanowire conductivity with deionized water and mineral oil as two different working fluids. The use of a higher permittivity fluid such as water extends the measurement range to more conductive particles (*cf.* eq 2), while larger bandwidth electronics increases the measurable range in both directions with the use of a low-conductivity fluid such as

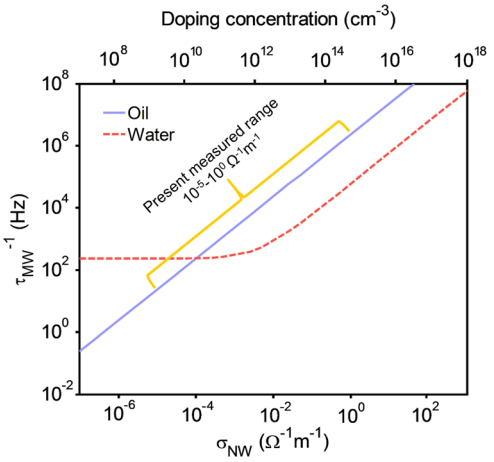

Figure 5. Measurable electrical-conductivity ranges and expected crossover frequency as a function of electrical conductivity of nanowires for different liquid media. The measurable range of nanowire conductivities depends on choice of fluid and bandwidth of experimental apparatus.

mineral oil. Miniaturization of the electro-orientation experimental apparatus (*e.g.*, in a microfluidic device) may also make it easier to apply the high frequencies required to extend the measurement range to higher conductivities.

One inherent limitation of the electro-orientation method is that it relies upon the optical visualization of individual nanowires. One-dimensional nanomaterials as small as individual single-walled carbon nanotubes (~1 nm × 500 μm) can be optically visualized[14] and characterized with the electro-orientation technique. However, the sensitivity of the method to uncertainties in the particle aspect ratio should be considered when the dimensions of very-small-diameter particles cannot be precisely resolved due to diffraction-limited imaging. The uncertainty in the measured electrical conductivity for an individual large-aspect-ratio particle is 1.8× the uncertainty in aspect ratio; hence, a 10% error in optically determined aspect ratio would result in an 18% error in the measured conductivity (see Supporting Information Figure S2). However, even if the measurement precision of an individual small-diameter nanowire is limited, it is still possible to accurately find the statistics of a nanowire ensemble. This can be done by independently measuring the aspect-ratio distribution of the nanowire ensemble (*e.g.*, using SEM or TEM) and then using linear error analysis to predict the exact conductivity distribution of the sample from electro-orientation measurements (see Supporting Information Figure S3). In this manner, it is possible to find statistics such as the mean, standard deviation, and higher moments of the conductivity distribution of a nanowire sample, as long as the aspect-ratio distribution of the sample can be found. Furthermore, the method need not solely rely on optical microscopy to image the electric-field-induced alignment of nanowires or nanotubes. Any method of measuring the transient electro-orientation rate can be used, for example, polarimetry[12,13] at the appropriate wavelengths that are sensitive to nanoparticle alignment.

The analysis embodied in eqs 1 and 2 assumes homogeneous electrical properties for the nanowires, and, thus, the presence of a surfactant could affect the measured conductivity. For the very low concentrations of the nanowires that we tested (since we are visualizing individual nanowires), a surfactant was not required. The need for a surfactant can also be minimized by choosing the appropriate solvent depending on the nanowire or nanotube. However, the choice of solvent may also affect the measurements in terms of electrolysis and induced-charge electro-osmosis.[17,21,22] From a theoretical standpoint, it may be possible to model surface effects on a nanowire with a core−shell model and extract the intrinsic conductivity, similar to what has been done for cells.[30] One could also measure nanowires of different diameters to distinguish between surface and bulk effects and then back calculate the bulk conductivity.[31,32] Thus far, however, we have avoided surfactants and considered the properties of the nanowire to be homogeneous.

CONCLUSION

We have demonstrated the use of solution-based electro-orientation spectroscopy to efficiently characterize the electrical properties of 1D nanomaterials. The method not only is able to quantitatively measure the electrical transport properties of a variety of insulating and semiconducting nanowires, but can also determine the statistics of a heterogeneous sample of very small diameter nanowires or nanotubes. Using the method, we characterize Si nanowires with different surface-state densities, as well as as-received, commercially purchased Al_2O_3 and TiO_2 nanowires. For n-type Si nanowires fabricated by metal-assisted chemical etching, we find significant variability within the same wafer and a strong dependence of electrical conductivity on surface states, with surface passivation increasing the effective conductivity by more than an order of magnitude. This indicates that active carrier concentration is being depleted by surface traps in the as-produced Si nanowires. Comparison between electro-orientation and direct STM measurements show good agreement for both as-produced and passivated Si nanowires. The solution-based electro-orientation method may have unique advantages for building nanowire- or nanotube-based functional nanodevices[33−37] because it is compatible with other solution-based methods for nanowire alignment and assembly, including electrophoresis,[38] dielectrophoresis,[15,16,39] and flow control.[33,40] We anticipate that this new method, by making the efficient statistical characterization of 1D nanomaterials widely accessible, will ultimately enable better understanding of

process−structure−property relationships and be an important tool for nanomanufacturing of functional devices utilizing postgrowth sorted and assembled nanowires.

METHODS

Nanowires. We have used commercially available Al_2O_3 (Pardam Nanotechnology) and TiO_2 nanowires (Novarials), as well as Si nanowires that we fabricated ourselves. The 1D nanomaterials were typically 50−300 nm in diameter and 5−30 μm in length. Silicon nanowires were synthesized by a metal-assisted chemical-etching method described in detail elsewhere.[20] Briefly, an n-type Si wafer ((2.0−3.3) × 10 Ω^{-1} m^{-1}) was washed with ethanol, acetone, and DI water for 10 min in each solvent. The wafer was then immersed in H_2SO_4 (97%) and H_2O_2 (35%) in a volume ratio of 3:1 for 30 min at room temperature and then etched with 5% HF aqueous solution for 3 min at room temperature. The Si wafer was next placed into a Ag-coating solution containing 4.8 M HF and 0.005 M $AgNO_3$, which was slowly stirred for 1 min. After a uniform layer of Ag nanoparticles coated the Si wafer, the wafer was rinsed with DI water to remove the excess Ag^+ ions and then immersed in an etchant composed of 4.8 M HF and 0.2 M H_2O_2. After 3 h of etching in the dark at room temperature, the wafer was repeatedly rinsed with DI water and then immersed in dilute HNO_3 (1:1 v/v) for 60 min to dissolve the Ag catalyst. The wafer was washed with 5% HF again for 1 min to remove the oxide layer and then cleaned with DI water and dried under N_2 flow. As-produced Si nanowires were in some cases treated with dry-oxygen passivation (950 °C for 15 min) immediately before testing to modify the surface states. Both as-produced and passivated Si nanowires were vacuum annealed at 350 °C for several hours prior to testing. The commercial nanowires were used as-received.

Electro-orientation-Spectroscopy Apparatus. A device consisting of parallel electrodes on a glass substrate was constructed by affixing stainless-steel wires atop a glass slide with a spacing of 0.5 mm horizontally and 1 mm vertically (Figure 2a). An inverted optical microscope (Olympus IX71, Olympus Corp.) with a 40× objective lens (Olympus LUCPLFN 40×, N.A. 0.6, Olympus Corp.) and a high-speed monochrome CCD camera (pco.edge sCMOS, PCO AG) was used to record the nanowire rotation. Uniform ac electric fields of different frequencies were applied to the sample by an arbitrary waveform generator (Agilent 33120A, Agilent Technologies Inc.) connected to a high-frequency amplifier (Trek 2100 HF, Trek Inc.). Mineral oil (Drakeol 7 LT mineral oil, Calumet Specialty Products and Partners, L.P.) was chosen to suspend the 1D nanomaterials because of its low conductivity and high viscosity, which reduced particle disturbances due to ac electro-osmotic background flow, as well as induced-charge electro-osmotic flow on the particles. Image analysis of nanowire alignment under different ac fields was performed using code developed in MATLAB (Mathworks Inc.).

Transport Measurements by Four-Probe STM. Transport measurements were carried out at room temperature with a four-probe STM (Unisoku/RHK, Unisoku Co., Ltd.) as described in detail elsewhere.[4] Briefly, a drop of nanowire/ethanol dispersion was placed on a SiO_2-coated Si substrate and then introduced into the UHV system (base pressure <2× 10^{-10} Torr). The samples were first annealed at a temperature of 250−300 °C and then transferred to the characterization platform containing four STM probes and an *in situ* SEM. Probes were made *via* electrochemically etched tungsten. Contacts between probes and nanowires were established with the guidance of the STM scanner and SEM image. The transport measurements were performed with a sourcemeter (Keithley 6430, Keithley Instruments Inc.).

Image Analysis and Conductivity Measurement. By using a code developed in MATLAB (Mathworks Inc.), an ellipse is fitted to nanowires in the recorded time-lapse image series to obtain the nanowire orientation. The maximum alignment rate (with nanowires at 45° relative to the electric field) at every measured frequency is plotted to observe the crossover frequency behavior (Figure 3a). Least-squares fitting is used to obtain the crossover in alignment rate at different frequencies in the form of $\Omega = 1/(1 + (\omega/\omega_{crossover})^2)$ where Ω is the normalized alignment rate, ω is the frequency of the applied electric field, and $\omega_{crossover}$ is the fitted crossover frequency. The nanowire conductivity can be extracted by substituting the crossover frequency value into eq 2, along with the permittivity of fluid and the aspect ratio of the particle.

Conflict of Interest: The authors declare no competing financial interest.

Acknowledgment. This work was supported in part by the National Science Foundation (CBET 0644719) and by the Chemical and Biological Technologies Department of the Defense Threat Reduction Agency (DTRA-CB) *via* grant BA12PHM123 in the "Dynamic Multifunctional Materials for a Second Skin D[MS]2" program (J.W.S. and C.A.). Four-probe STM measurements (C.D., S.M.H., and A.-P.L.) were conducted at the Center for Nanophase Materials Sciences, which is sponsored at Oak Ridge National Laboratory by the Scientific User Facilities Division, Office of Basic Energy Sciences, U.S. Department of Energy.

Supporting Information Available: Additional information available includes supporting video and figures and theoretical analysis of electro-orientation torque and alignment rate, discussion of additional factors that may affect NW conductivity, estimation of Si-nanowire dopant concentration and number of surface states, and prediction of conductivity statistics by linear error analysis. The Supporting Information is available free of charge on the ACS Publications website at DOI: 10.1021/acsnano.5b01170.

REFERENCES AND NOTES

1. Koenraad, P. M.; Flatté, M. E. *Nat. Mater.* **2011**, *10*, 91–100.
2. Qin, S.; Kim, T.-H.; Zhang, Y.; Ouyang, W.; Weitering, H. H.; Shih, C.-K.; Baddorf, A. P.; Wu, R.; Li, A.-P. *Nano Lett.* **2012**, *12*, 938–942.
3. Roduner, E. *Chem. Soc. Rev.* **2006**, *35*, 583–592.
4. Kim, T.-H.; Wang, Z.; Wendelken, J. F.; Weitering, H. H.; Li, W.; Li, A.-P. *Rev. Sci. Instrum.* **2007**, *78*, 123701.
5. Gu, W.; Choi, H.; Kim, K. K. *Appl. Phys. Lett.* **2006**, *89*, 253102.
6. Perea, D. E.; Hemesath, E. R.; Schwalbach, E. J.; Lensch-Falk, J. L.; Voorhees, P. W.; Lauhon, L. J. *Nat. Nanotechnol.* **2009**, *4*, 315–319.
7. Perea, D. E.; Allen, J. E.; May, S. J.; Wessels, B. W.; Seidman, D. N.; Lauhon, L. J. *Nano Lett.* **2006**, *6*, 181–185.
8. Allen, J. E.; Perea, D. E.; Hemesath, E. R.; Lauhon, L. J. *Adv. Mater.* **2009**, *21*, 3067–3072.
9. Koren, E.; Rosenwaks, Y.; Allen, J.; Hemesath, E.; Lauhon, L. *Appl. Phys. Lett.* **2009**, *95*, 092105.
10. Amit, I.; Givan, U.; Connell, J. G.; Paul, D. F.; Hammond, J. S.; Lauhon, L. J.; Rosenwaks, Y. *Nano Lett.* **2013**, *13*, 2598–2604.
11. McCartney, M.; Gribelyuk, M.; Li, J.; Ronsheim, P.; McMurray, J.; Smith, D. J. *Appl. Phys. Lett.* **2002**, *80*, 3213–3215.
12. Bubke, K.; Gnewuch, H.; Hempstead, M.; Hammer, J.; Green, M. L. *Appl. Phys. Lett.* **1997**, *71*, 1906–1908.
13. Brown, M. S.; Shan, J. W.; Lin, C.; Zimmermann, F. M. *Appl. Phys. Lett.* **2007**, *90*, 203108.
14. Duggal, R.; Pasquali, M. *Phys. Rev. Lett.* **2006**, *96*, 246104.
15. Fan, D.; Zhu, F.; Cammarata, R.; Chien, C. *Appl. Phys. Lett.* **2004**, *85*, 4175–4177.
16. Edwards, B.; Engheta, N.; Evoy, S. *J. Appl. Phys.* **2007**, *102*, 024913.
17. Arcenegui, J. J.; García-Sánchez, P.; Morgan, H.; Ramos, A. *Phys. Rev. E* **2013**, *88*, 063018.
18. Jones, T. B. *Electromechanics of Particles*; Cambridge University Press, 2005.

19. Morgan, H.; Green, N. G. *AC Electrokinetics: Colloids and Nanoparticles*; Research Studies Press, 2003.
20. Peng, K.; Hu, J.; Yan, Y.; Wu, Y.; Fang, H.; Xu, Y.; Lee, S.; Zhu, J. *Adv. Funct. Mater.* **2006**, *16*, 387–394.
21. Rose, K. A.; Meier, J. A.; Dougherty, G. M.; Santiago, J. G. *Phys. Rev. E* **2007**, *75*, 011503.
22. Fan, D.; Zhu, F. Q.; Xu, X.; Cammarata, R. C.; Chien, C. *Proc. Natl. Acad. Sci. U.S.A.* **2012**, *109*, 9309–9313.
23. Squires, T. M.; Bazant, M. Z. *J. Fluid Mech.* **2004**, *509*, 217–252.
24. LeMieux, M. C.; Roberts, M.; Barman, S.; Jin, Y. W.; Kim, J. M.; Bao, Z. *Science* **2008**, *321*, 101–104.
25. Tanaka, T.; Jin, H.; Miyata, Y.; Fujii, S.; Suga, H.; Naitoh, Y.; Minari, T.; Miyadera, T.; Tsukagoshi, K.; Kataura, H. *Nano Lett.* **2009**, *9*, 1497–1500.
26. Chen, F.; Wang, B.; Chen, Y.; Li, L.-J. *Nano Lett.* **2007**, *7*, 3013–3017.
27. Zheng, M.; Jagota, A.; Semke, E. D.; Diner, B. A.; McLean, R. S.; Lustig, S. R.; Richardson, R. E.; Tassi, N. G. *Nat. Mater.* **2003**, *2*, 338–342.
28. Arnold, M. S.; Green, A. A.; Hulvat, J. F.; Stupp, S. I.; Hersam, M. C. *Nat. Nanotechnol.* **2006**, *1*, 60–65.
29. Krupke, R.; Hennrich, F.; Löhneysen, H. v.; Kappes, M. M. *Science* **2003**, *301*, 344–347.
30. Miller, R. D.; Jones, T. B. *Biophys. J.* **1993**, *64*, 1588–1595.
31. Simpkins, B.; Mastro, M.; Eddy, C., Jr.; Pehrsson, P. *J. Appl. Phys.* **2008**, *103*, 104313.
32. Gurwitz, R.; Shalish, I. *Nanotechnology* **2011**, *22*, 435705.
33. Cui, Y.; Wei, Q.; Park, H.; Lieber, C. M. *Science* **2001**, *293*, 1289–1292.
34. Law, M.; Greene, L. E.; Johnson, J. C.; Saykally, R.; Yang, P. *Nat. Mater.* **2005**, *4*, 455–459.
35. Li, Y.; Qian, F.; Xiang, J.; Lieber, C. M. *Mater. Today* **2006**, *9*, 18–27.
36. Li, M.; Bhiladvala, R. B.; Morrow, T. J.; Sioss, J. A.; Lew, K.-K.; Redwing, J. M.; Keating, C. D.; Mayer, T. S. *Nat. Nanotechnol.* **2008**, *3*, 88–92.
37. Morrow, T. J.; Li, M.; Kim, J.; Mayer, T. S.; Keating, C. D. *Science* **2009**, *323*, 352–352.
38. Yu, K.; Lu, X.; Yi, J.; Shan, J. *Electrophoresis-Based Motion Planning and Control of a Nanowire in Fluid Suspension*; IEEE International Conference on Automation Science and Engineering (CASE), 2013; **2013**; pp 819−824.
39. Freer, E. M.; Grachev, O.; Duan, X.; Martin, S.; Stumbo, D. P. *Nat. Nanotechnol.* **2010**, *5*, 525–530.
40. Mathai, P. P.; Carmichael, P. T.; Shapiro, B. A.; Liddle, J. A. *R. Soc. Chem. Adv.* **2013**, *3*, 2677–2682.